CONSTRUCTION
E-ISSN: 2785-8731
VOLUME 6, ISSUE 1, 2026, 127 - 143
DOI: https://doi.org/10.15282/construction.v6i1.13574

RESEARCH ARTICLE

Correlating geophysical anomalies with subsurface lithology: Insights into gold mineralisation

Ooi Cheng Wee[1], Mohd Fakhrurrazi Ishak[1]*, Solahuddin Daud[1], Puteri Izrina Ismi[1], Yusra Aulia Sari[2]

[1]Faculty of Civil Engineering Technology, Universiti Malaysia Pahang Al-Sultan Abdullah, Lebuh Persiaran Tun Khalil Yaakob, 26300 Kuantan, Pahang, Malaysia
[2]Civil Engineering Program, Universitas Internasional Batam, Baloi-Sei Ladi, Jl. Gajah Mada, Tiban Indah, Kec. Sekupang, Kota Batam, Kepulauan Riau 29426 Batam, Indonesia

Abstract - Accurate delineation of gold mineralization in deeply weathered tropical terrains requires the integration of indirect geophysical data with direct subsurface observations. Electrical resistivity imaging (ERI) and induced polarization (IP) are widely used in mineral exploration; however, interpretation is often limited by non-uniqueness without borehole validation. This study evaluates the reliability of combined resistivity and induced polarization (Res-IP) methods for identifying sulphide-associated gold mineralization in the Central Belt of Peninsular Malaysia (CBPM) through correlation with borehole lithological data. The investigation was conducted in Jeli, Kelantan, a known gold-bearing region, using two intersecting 400 meters survey lines (SL-1 and SL-2) acquired with 61 electrodes at 5 to 10 meters Schlumberger spacing to generate two-dimensional (2D) Res-IP models. Boreholes Y (BH-Y) and Z (BH-Z) were drilled along SL-1 to validate geophysical anomalies, with detailed geological logging performed at 1.5 meters intervals to document lithology, alteration, quartz veining, and sulphide occurrence. The results reveal a consistent geophysical signature characterized by low resistivity (<100 Ωm) and high chargeability (>100 msec), indicative of disseminated to vein-hosted sulphides. These signatures correlate directly with quartz–sulphide vein intersections at depths of 70 to 72 meters in BH-Z and 102 to 102.6 meters in BH-Y, confirming subsurface structural and mineralogical continuity. This study establishes calibrated resistivity–chargeability thresholds for sulphide-bearing formations in tropical Malaysian geology, improving ERI interpretive confidence in highly weathered environments. The findings highlight the value of integrated geophysical and geological approaches for enhancing drill targeting and reducing exploration uncertainty in gold-prospective regions of Malaysia.

Article History
Received : 1 December 2025
Revised : 6 January 2026
Accepted : 19 February 2026
Published : 6 August 2026

Keywords
Geophysical anomalies
Electrical resistivity imaging
Induced polarization
Borehole lithology
Gold mineralization

1. Introduction

Malaysia recognises its abundance of mineral resources, which significantly contribute to national income, industrial development, and foreign investment, particularly in the mining and materials processing sectors. Among these resources, materials such as gold hold a prominent position due to their economic value, not only as natural resources but also as multifaceted materials that provide economic stability and attract investment. The state of Kelantan, particularly in the Central Belt of Peninsular Malaysia (CBPM), has long been synonymous with gold mineral wealth [1]-[3], offering substantial potential for exploration and extraction activities. The documented occurrences of gold deposits in this region have created opportunities for stakeholders in the mining industry to intensify efforts toward systematic exploration and sustainable exploitation of these resources [4]. Building on earlier discoveries, subsequent research has identified more than 30 promising gold exploration zones by integrating geochemical analyses [5], geological and geophysical assessments [6] - [7], and comprehensive datasets from existing mining operations [8]. According to previous studies, the geological and tectonic framework of the Kelantan region indicates the presence of gold deposits within a belt classified as mesothermal lodes, characteristic of orogenic-type mineralisation [2], [9]-[11]. As stated by Endut et al. [11] and Pour and Hashim [12], the gold mineralisation is chiefly concentrated within low-grade volcano-sedimentary units and is structurally controlled by steeply inclined fault systems. In addition to Kelantan, substantial gold reserves are also thought to occur in the neighbouring state of Pahang [7], which lies within the same CBPM recognised as Malaysia's primary metalloorganic corridor. However, the process of obtaining gold from subsurface deposits is inherently complex. It requires a series of integrated geological and geophysical investigations to accurately identify and assess the presence and viability of gold-bearing formations. Such efforts are crucial for ensuring that resource development aligns with both economic objectives and environmental sustainability, thereby contributing to Malaysia's broader goals of sustainable mineral resource management and economic diversification.

Geophysical methods have long been integral to mineral exploration, with numerous studies demonstrating their effectiveness in mapping subsurface conditions and identifying zones of economic mineralisation. Electrical resistivity imaging (ERI) and induced polarisation (IP) are among the most applied techniques, particularly in gold exploration, due to their sensitivity to the electrical responses of sulphide-bearing or metal-rich formations. Previous research has shown that mineralised zones often manifest as low-resistivity and high-chargeability anomalies, enabling effective delineation of potential ore-bearing structures. Studies utilising combined resistivity–induced polarisation (Res-IP) surveys have further demonstrated their capability to detect variations in lithology, porosity, moisture content, and the presence of

***CORRESPONDING AUTHOR | Mohd Fakhrurrazi Ishak** | ✉ fakhrurrazi@umpsa.edu.my

disseminated sulphide minerals, as the IP response highlights the capacity of geological materials to store electrical charge temporarily. Numerous investigations of gold prospects in structurally complex terrains have also confirmed that Res-IP methods can reliably map fault zones, shear-related mineralisation, and concealed ore bodies, providing essential subsurface constraints to guide drilling programs and refine exploration targets. Overall, the findings from these studies underscore the value of integrated geophysical approaches in improving the accuracy, efficiency, and cost-effectiveness of gold mineral exploration. Zaid et al. [13] also carried out a geophysical survey in Gua Musang, Kelantan, utilising a combination of Res-IP methods to map potential conductive zones associated with sulphide mineralisation. The study identified low-resistivity, high-chargeability zones indicative of gold-bearing sulphides at depths ranging from 25 to 135 meters (m). Kayode et al. [7] research contributes to this body of work by applying integrated Res-IP surveys alongside regional geological mapping and three-dimensional (3D) geographic information system analysis across the CBPM. Their findings confirm that chargeability anomalies, typically associated with disseminated sulphides rather than gold itself, are effective indicators of potential mineralised zones. The study successfully delineated sulphide-rich bodies at depth (approximately 200-300 m), exhibiting characteristic geophysical signatures, including chargeability values <45 ms and resistivity of around 50 Ωm, consistent with previous interpretations of sulphide-hosted mineral systems. Arifin et al. [8] research represents a significant contribution to mineral exploration studies in Malaysia, particularly through the application of integrated Res-IP surveys to delineate gold mineralisation zones. Conducted across twenty-one (21) survey lines within the Felda Chiku 3 area of Gua Musang, Kelantan, the study generated detailed resistivity and chargeability models that successfully identified potential sulphide-rich mineralised zones at depths of approximately 25-50 m. The generated anomalies are characterised by low resistivity and high chargeability, enabling clear mapping of structurally controlled mineralisation trends. The spatial distribution of these anomalies aligns well with the underlying geological setting, which comprises phyllite, schist, and quartz-veined lithologies commonly associated with hydrothermal gold deposits.

Building on the recent research works of Zaid et al. [13], Kayode et al. [7], and Arifin et al. [8], who successfully applied Res-IP methods for gold mineralisation prospecting in Malaysia, particularly in CBPM, their findings collectively provide a foundation and motivation for the present research, catalysing further investigation using similar geophysical approaches. In addition to research carried out in Malaysia, several international studies have demonstrated the effectiveness of integrated geophysical methods for mineral exploration. For example, Sono et al. [14] applied a combined Res-IP survey to map prospective gold-bearing zones in the Mopolo region of Southeast Botswana. In Brazil, Lenhare and Moreira [15] used IP and direct-current resistivity techniques to support strategic planning for a sulphide-rich mining operation. Likewise, Mashhadi et al. [16] re-evaluated Res-IP datasets to improve the identification of gold mineralisation targets in the Zarzima area of Iran. By combining Res-IP data to generate detailed geophysical anomalies, the method can be applied in multiple ways to characterise subsurface structures with greater precision [15]-[22]. This integrated approach allows for the identification of lithological boundaries, the detection of fracture and fault zones, the mapping of weathered or altered units, and the recognition of potential sulphide-bearing or mineralised bodies [24]-[25].

However, all researchers emphasised the need to validate geophysical anomaly interpretations through borehole drilling to establish a reliable correlation between the two independent datasets and refine the delineation of gold deposits in their study area. While geophysical methods provide valuable subsurface anomalies, their interpretations require ground-truth validation through direct observations such as borehole lithology or core samples [26]-[27]. Borehole data help constrain geophysical inversion models, refine resistivity thresholds, and confirm the geological significance of anomalies [28]. Several studies have demonstrated that integrating geophysical anomalies with borehole lithology significantly enhances the accuracy of subsurface characterisation [29]-[31]. According to Nizam et al. [32], the resistivity anomalies showed strong consistency with borehole logging data of the subsurface materials in Terendak, Melaka. They conducted an ERI method, supported by borehole drilling, which clearly identified the weathered and fractured zones within the bedrock, and the borehole lithological records later confirmed these zones. Kieu and Kepic [26] introduced an inversion approach that integrates geophysical data with multiple borehole attributes using fuzzy clustering. By incorporating lithology, assays, wireline logs, and core data, the method produces subsurface models that better match geophysical responses and drilling evidence. This integration improves inversion accuracy and enhances the delineation of mineralised zones.

Validating geophysical anomalies, such as resistivity survey imaging, with borehole drilling is essential because Res-IP provides indirect geophysical signals that require ground-truth confirmation for accurate interpretation of subsurface lithology and mineralisation. Electrical resistivity measures resistivity contrasts related to rock and mineral properties; however, similar resistivity anomalies can stem from various geological factors, such as clay content, water saturation, or fractured zones, which may or may not indicate gold mineralisation. Additionally, borehole drilling physically samples the subsurface, confirming the presence, type, and grade of mineralisation, thereby verifying and calibrating the geophysical anomalies observed in resistivity data. This validation reduces false positives and enhances confidence in using the Res-IP method for targeting drilling sites, particularly in complex terrains such as those in CBPM. In mineral exploration, a geophysical survey such as ERI serves as a cost-effective, non-invasive tool for mapping broad subsurface features and guiding drilling. In terms of drilling, it is expensive and limited in spatial coverage, so relying solely on ERI without validation risks misinterpretation and wasted resources. Validated ERI results enable better delineation of mineralised zones, optimise drill targeting, and increase exploration efficiency. This comprehensive approach bridges the fields of geophysics and geology, enabling more reliable subsurface modelling, assessment of ore continuity, and more accurate resource estimation.

Despite the widespread application of resistivity and induced polarisation methods in gold exploration, the interpretation of geophysical anomalies in tropical environments remains highly uncertain due to deep weathering and the non-uniqueness of electrical responses. In Malaysia, most Res-IP studies interpret low-resistivity and high-chargeability anomalies as indicators of mineralisation without direct borehole validation, resulting in the absence of calibrated geoelectrical thresholds specific to local geological conditions. This study hypothesises that sulphide-associated gold mineralisation in the CBPM produces characteristic resistivity and chargeability responses that can be quantitatively constrained through borehole correlation.

Accordingly, this research aims to examine the relationship between Res-IP anomalies and borehole-confirmed subsurface lithology in the Jeli gold prospect area, and (ii) evaluate the extent to which borehole calibration improves the reliability of Res-IP interpretations in distinguishing mineralised zones from barren conductive units in tropical terrains. To address this gap, the present study integrates intersecting 2-D Res-IP survey lines with two strategically drilled boreholes to directly correlate geophysical anomalies with logged subsurface lithology. This approach provides the first borehole-calibrated geoelectrical dataset from the CBPM, enabling the establishment of Malaysian-specific thresholds for sulphide-associated gold mineralisation. The study advances existing knowledge by enhancing the interpretive accuracy of geophysical methods in highly weathered tropical environments and by providing a reproducible framework for reducing uncertainty in drill targeting. Therefore, this study aims to address these limitations by correlating a geophysical anomaly with Res-IP and borehole lithology data from the Jeli, Kelantan, gold prospect area. Through this approach, the research seeks to (i) refine resistivity and chargeability ranges representative of gold-bearing formations, (ii) evaluate the reliability of geophysical interpretations through ground-truth validation, and (iii) compare geophysical anomalies and borehole-confirmed subsurface materials.

2. Materials and Methods

As shown in Figure 1, this study follows a structured methodological framework. The process begins with identifying a site with strong potential for mineral occurrence, followed by a geophysical survey that includes electrical resistivity imaging and borehole drilling. ERI datasets are processed and analysed using specialised software, and detailed lithological logs are generated for each borehole. A subsequent comparison of the two interpretations enables evaluation of their correlation and reliability.

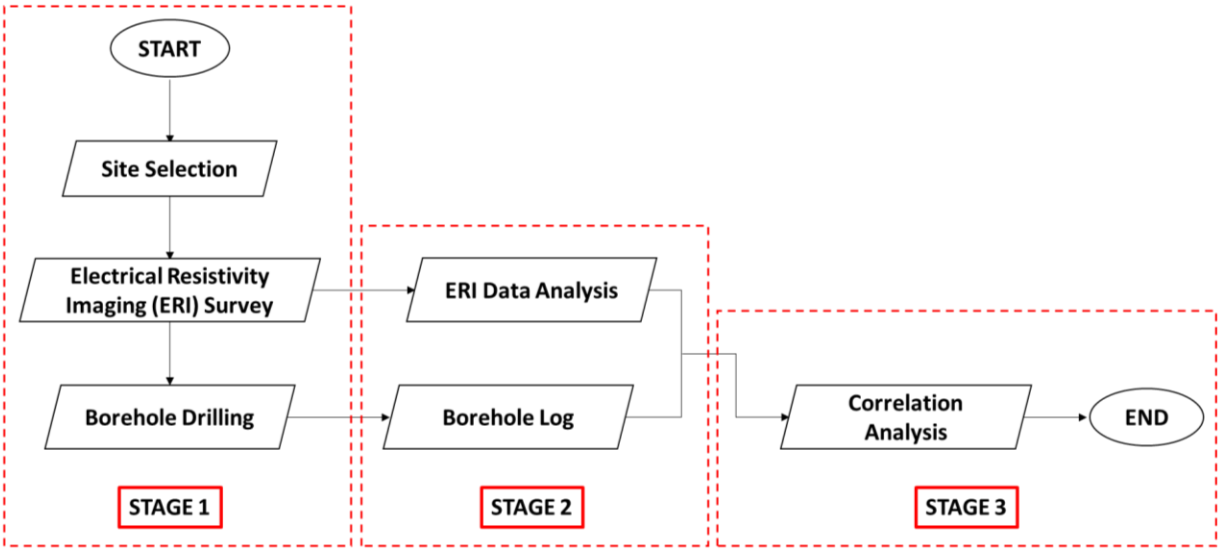

Figure 1. Methodological framework illustrating the sequential workflow of the study

2.1 Delineation of Gold Mineralisation Zones

The study area is in Jeli, Kelantan, within the CBPM, a locality chosen for its long-standing and contemporary significance in mineral resource development, as depicted in Figure 2(a). The geophysical survey line and borehole drilling site are positioned at 5° 59' 0.1284" N and 100° 40' 53.9256" E, corresponding to Kertau RSO coordinates of 662249 N and 299777 E. The total area encompasses approximately 130 acres. Jeli forms one of the ten administrative districts in Kelantan and is in the western part of the state. Its strategic position is near the Kelantan–Perak state boundary and the Malaysia–Thailand international border. The Jeli district, covering approximately 2,552 km², comprises three (3) distinct geomorphological zones: i) lowlands; ii) hills; and iii) mountainous terrain [33]. Jeli district is blessed with a wealth of beautiful geological landforms, unique geological phenomena, and valuable earth materials. The Jeli district lies at the foot of the Main Range of Peninsular Malaysia, which forms part of the peninsula's dominant backbone. As stated by Heng et al. [34], the general geology of Kelantan consists of three major rock types: sedimentary, metasedimentary, and granitic intrusion rocks. The geology of this area is characterized by a complex framework primarily composed of three (3) main rock types: i) Triassic sedimentary rocks of the Gunong Rabong Formation, which include shale, siltstone, sandstone, and limestone; ii) Permian sedimentary rocks of the Gua Musang Formation, consisting of phyllite, slate, sandstone, and limestone; and iii) locally extensive granitic rocks that are acid intrusive in nature [33]-[34]. The general geology of the Kelantan and Jeli districts is comprehensively illustrated in Figure 2(c) and Figure 2(d). This diverse lithological assemblage has been significantly influenced by tectonic activities during the Palaeozoic and Mesozoic eras, resulting in a complex network of geological structures, including folding, jointing, and faulting. These structural features dominate the local landscape, with the principal structural trends-oriented northwest-southeast and northeast-southwest, reflecting the dynamic geological processes that have shaped the region and contributed to its mineralisation potential, including gold. The geochemical, geological, structural geology, and geophysical data from previous studies indicate that most gold mineralisation in Kelantan is associated with Triassic and Permian metasedimentary rocks [33], [35]-[37].

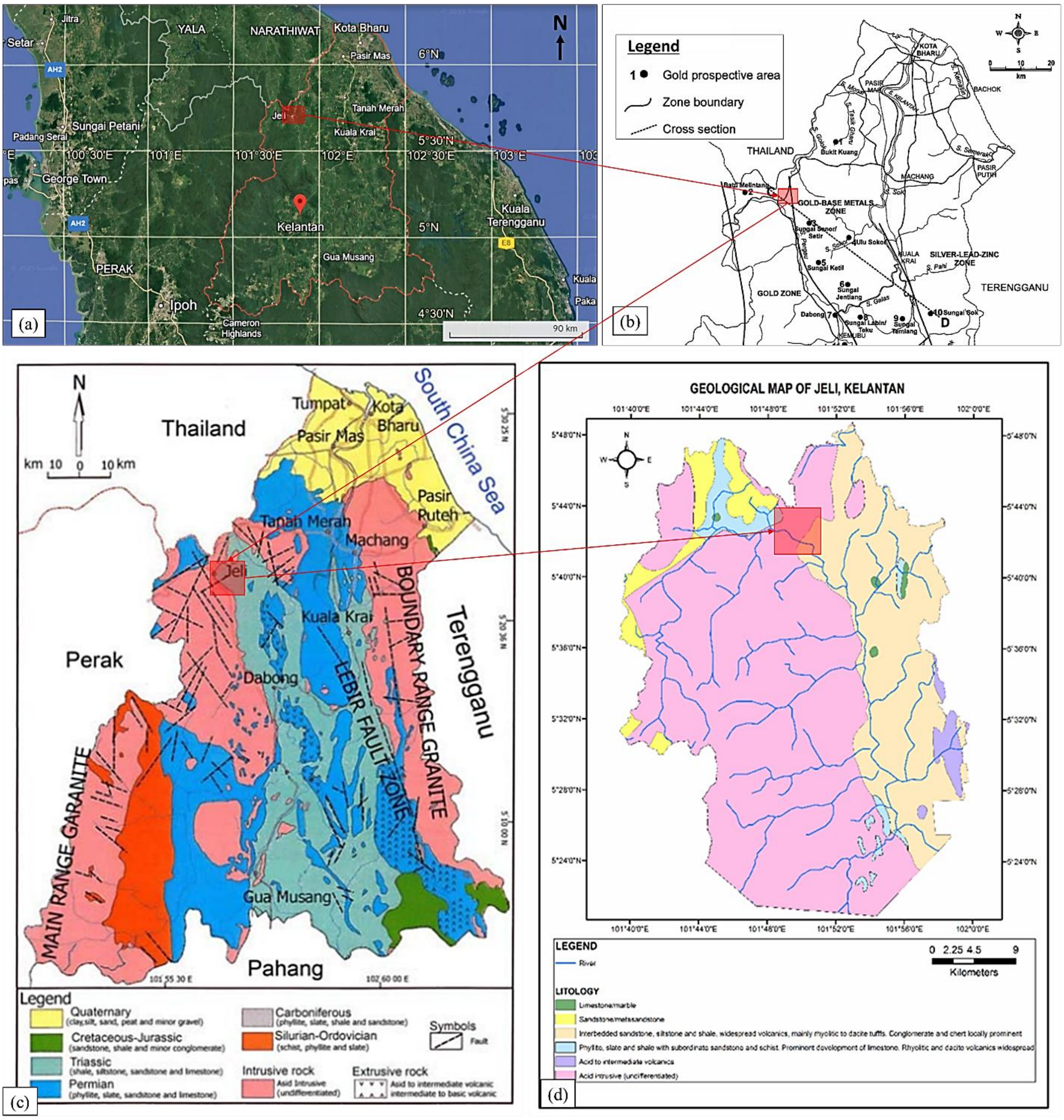

Figure 2. (a) Map of Kelantan State, Malaysia, showing the location of the study area; (b) Modified map illustrating the distribution of gold mineralisation across the western side of Kelantan [34] (c) Geological map of Kelantan, Malaysia, highlighting the main lithologies for the whole state [45]; (d) Geological map of Jeli district [36]

Gold mineralisation in western Kelantan is primarily concentrated in the CBPM, with key locations in the Jeli, Tanah Merah, and Gua Musang districts. Gold mineralisation in Kelantan is primarily concentrated in the central region of the state, bounded by the Stong Igneous Complex and Seting Granite to the west, the Kemahang Granite to the north, and the Boundary Range Granite to the east [9]. Figure 2(b) illustrates the distribution of gold mineralisation across Kelantan. The primary gold mineralisation deposits in the CBPM can be classified into three (3) types: i) quartz veins, ii) massive sulphides, and iii) skarn [40]. Among these, the most prominent gold mineralisation occurs in quartz veins. Two (2) distinct styles of gold mineralisation have been identified: i) gold associated with sulphide minerals; and ii) gold associated with base metals and carbonate veins [1]. Hassan and Purwanto [37] stated that gold mineralisation in quartz veins is distributed across a broad region, extending from Batu Melintang and Panggung Lalat in Kelantan, through Tersang, Selinsing, Kecau Tui, Penjom, and Raub in Pahang, to Gunung Ledang in Johor. Several researchers have reported that, in northern Kelantan, gold mineralisation is typically associated with hydrothermal quartz vein systems, skarn deposits, and volcanogenic massive sulphides [39]-[42]. A regional geochemical survey for gold conducted by the Malaysian authorities across the Central Belt of North Pahang and Kelantan identified a 20-km-wide, north–south-trending gold-mineralised zone extending from the Raub–Kuala Medang–Lipis–Merapoh region in Pahang to the Ulu Sokor–Sungai Sok–Katok Batu–Pulai area in Kelantan. Gold mineralisation within the Central Gold Belt is generally classified as low-mesothermal lode-type, reflecting the prevailing tectonic and geological framework of the region. Apart from the Jeli district, Ulu Sokor in the Tanah Merah district is also well known for its gold deposits. The area of Sokor, Tanah Merah, is primarily composed of the Taku Schist Formation and the Kemahang Granite [34], [42]. The Taku Schist is recognised as a product of hydrothermal or regional metamorphism, characterised by an extensive body of predominantly pelitic schist. According to Hutchinson and Tan [41], the lithology of the Taku Schist Formation is predominantly composed of metamorphic rocks. The main constituent of this formation is mica schist, which includes quartz-mica schist, mica-garnet schist, and quartz-mica-garnet schist. Additionally, other rock types found within the formation include amphibolite schist, quartz schist, and carbonate schist. A combination of geological, structural, and practical considerations guided the selection of survey locations for the two Res-IP lines. The CBPM is widely recognised for hosting hydrothermal gold deposits associated with quartz–sulphide vein systems; therefore, survey lines were strategically positioned across mapped structural lineaments interpreted as potential fluid pathways. The study area is also a well-established zone of mineral exploration and extraction in Kelantan, further supporting its suitability for focused investigation.

2.2 Setup, Equipment, and Data Processing

The ERI geophysical survey is one of several electrical resistivity techniques used in geophysical engineering to detect variations in subsurface electrical resistivity [44]-[46]. The ERI method was used in this study because it enables the identification of materials associated with gold mineralisation, such as quartz veins within massive sulphides, and provides sufficient depth for mineral exploration [8], [15]. The apparatus involved in the geophysical survey comprises three (3) major parts: a record, an inducer, and a source [48]. To obtain the ERI properties of the subsurface geological lithologies, a direct current (DC) supplied by a 12-volt battery was used to power the ABEM Terrameter LS2 resistivity meter arrangement, which features an inbuilt microprocessor. The study comprises three main phases: (i) desk-based investigation, (ii) field data collection, and (iii) analytical processing. The desk-based investigation involves gathering essential background information on the study area using maps, geological reports, and geoheritage sources. This phase is crucial for establishing an accurate contextual foundation, particularly regarding the gold-mining activities and associated mineral resources that are prevalent in the Jeli District of Kelantan. A total of two (2) spread lines of the ERI method were carried out in the study area, known as Survey Line 1 (SL-1) and Survey Line 2 (SL-2). SL-1 and SL-2 were intentionally configured to intersect to facilitate data quality control, and the central point of both lines was located under the same site conditions. Both survey lines were established using 61 electrodes and 64 transmitters, with electrode spacings of 5 m for the inner spread and 10 m for the outer spread. Each line extended 400 m in length, and data acquisition followed the Schlumberger protocol, which provides dense near-surface coverage and sparser measurements at greater electrode spacings [47][49]. As illustrated in Figure 3, SL-1 was oriented east-northeast to west-southwest (ENE–WSW), while SL-2 extended north-northwest to south-southeast (NNW–SSE), perpendicular to SL-1. The “Start” and “End” points of each line correspond to 0 and 400 m, respectively. Electrode coordinates were determined using a handheld global positioning system (GPS) device, which calculated precise positions by triangulating satellite signals.

The orientations of SL-1 (ENE–WSW) and SL-2 (NNW–SSE) were deliberately chosen to intersect the dominant fracture and foliation trends identified through detailed surface geological mapping, thereby enhancing the likelihood of imaging structurally controlled mineralised zones. Borehole locations (BH-Y and BH-Z) were placed along SL-1 at anomaly positions identified in preliminary geophysical modelling to enable direct ground-truth validation of subsurface signatures. Collectively, these criteria ensured that the survey configuration maximised geological relevance, aligned with known structural controls on mineralisation, and enhanced the interpretive reliability of the resulting geophysical dataset. According to Loke and Barker [47], geoelectric prospecting measures the subsurface response to direct current by injecting current through electrodes and recording the resulting potential differences to determine the electrical properties of geological formations. As noted by Upadhyay et al. [48], the accuracy of these measurements depends on both the electrode configuration and the physical properties of the subsurface materials. The actual measurements were then carried out, and the field data were evaluated and analysed using RES2DINV software [46]. Furthermore, the Schlumberger arrays were used during data collection because fewer electrodes needed to be moved for each sounding, and the cable length for the potential electrodes was short. Schlumberger soundings also have higher resolution, greater probing depth, and require less time to deploy in the field. The unprocessed data obtained from the ERI field investigation were then analysed using the commercially available RES2DINV software [50]-[52] to create an inversion model that closely matched the simple subsurface structure. The 2D resistivity models of the subsurface were derived from interface data measured using the RES2DINV inversion code. The RES2DINV code can generate immediate designs from the resistivity input data using a smoothness-constrained least-squares method [48], [54]-[55]. According to Smith and Sjögren [52] and Marescot et al. [53], geoelectric prospecting methods operate by transmitting direct current into the subsurface through current electrodes and measuring the resulting electrical potential differences using potential electrodes. These measurements are then used to infer the electrical characteristics of the underlying geological formations. The effectiveness and output of such methods depend not only on the arrangement of the electrodes but also on how the physical properties of the materials respond to the applied electrical current [47], [55] - [57].

Electrical Resistivity Arrangements:					
Survey Line (SL)	Measure Mode	Total Length (m)	Coordinates of Survey Line		Cardinal Direction
			Start Point	End Point	
SL-1	Res, IP	400	5°40'43.70"N , 101°55'1.29"E	5°40'37.66"N , 101°54'50.11"E	ENE-WSW
SL-2	Res, IP	400	5°40'35.84"N , 101°54'58.65"E	5°40'46.83"N , 101°54'53.70"E	NNW-SSE

Borehole Drilling Arrangements:					
Borehole Point	Borehole Inclination (°)	Diameter Borehole (mm)	Maximum Depth of Penetration (m)	Coordinates of Borehole Point	Elevation (m)
BH-Y	70° to right	50	107.94	5°40'41.09"N , 101°54'55.43"E	105
BH-Z	70° to right	50	103.44	5°40'41.72"N , 101°54'55.98"E	117

Figure 3. Map of the electrical resistivity imaging survey profiles and borehole drilling locations within the study area, together with the corresponding survey parameters and borehole drilling information

The Res-IP method was employed to characterise subsurface materials and identify zones associated with gold mineralisation. This integrated geophysical technique measures both the electrical resistivity and chargeability of subsurface formations, providing complementary information on lithological variations and the presence of disseminated sulphide minerals. Induced polarisation (IP) also uses the same methods as the ERI techniques. The difference between resistivity and IP is that the IP method measures the apparent chargeability of the earth material, expressed in milliseconds (msec) or millivolts per Volt (mV/V) [60]. When the electrical current is injected into the ground, specific subsurface units, or metallic grains (a metal sulphide), which act as ions within rock bodies, may become electrically polarised (i.e., hold electrical charges). According to Reynolds [56], after the applied current is switched off, the polarised ground gradually decays to zero. The study of voltage decay over time is known as time-domain IP (TDIP). It is mainly used in applied geophysics for mineral exploration and exploitation programs. Although the combined Res-IP geophysical methods are effective for rapidly and qualitatively characterising subsurface geological materials, their interpretation can become considerably challenging in areas with complex geological settings. As noted by Arifin et al. [57], such terrains often contain intricate basement structures and heterogeneous lithologies, necessitating verification of geophysical interpretations against direct surface- or ground-based observations to enhance the accuracy and reliability of the results. The geophysical anomalies from the ERI survey in the study area, together with sufficient data, helped delineate and interpret the subsurface lithology, and borehole drilling validated the presence of massive sulphide gold deposits indicated by the Res-IP inversion models. Figure 3 illustrates the layout of the ERI survey profiles and borehole drilling locations within the study area, together with the associated survey parameters and borehole information used to support the geophysical investigation.

2.3 Subsurface Lithology Drilling and Borehole Logging

Before drilling, exploration data, including ERI anomaly results, were analysed to define target zones. In this study, we selected the deep rotary drilling method because it provides continuous penetration in a wide range of geological environments, offers efficient drilling rates, and is suitable for preliminary mineral exploration [59]. As noted by Cozzolino et al. [60], R drilling operations represent the most expensive component of mineral exploration. It particularly targets zones of low resistivity and high chargeability that indicate the presence of sulphide-rich and quartz-vein materials associated with gold mineralisation. The rotary drilling technique enabled efficient penetration through overburden and weathered bedrock, allowing for the recovery of continuous core samples for detailed lithological and mineralogical analysis. This approach provided direct subsurface verification of the geophysical interpretations, enhancing the accuracy of the geological model and confirming the correlation between the resistivity anomalies and actual gold-bearing quartz vein zones. This rotary-drilling exploration aimed to ground-truth the geophysical anomalies identified along the ERI survey line designated SL-1. The investigation drilled two boreholes (BH-Y and BH-Z) along the same straight line as the ERI profile to directly correlate subsurface resistivity responses with actual geological conditions and potential gold-bearing zones. Following the drilling methodology, the logging process systematically recorded the subsurface geological conditions encountered during drilling and correlated these observations with the ERI SL-1 geophysical profile. At each 1.5 m sampling interval, the examination of cuttings under appropriate lighting and magnification identified rock type, mineral content, alteration features, and textural variations. The study recorded observations, including quartz vein fragments, sulphide mineralisation, oxidation levels, and grain size, to characterise potential gold-bearing zones. All data entry used standardised logging sheets with unique identifiers corresponding to the borehole and SL-1 sample codes.

3. Results and Discussion

This study presents results in three basic elements in geophysical anomalies with subsurface lithology: (i) interpretation of electrical Res-IP data, (ii) lithological characterisation from borehole drilling and logging, and (iii) comparative analysis between geophysical anomalies and borehole-confirmed subsurface materials. Integrating these datasets provides a robust assessment of the subsurface framework and effectively delineates potential gold-bearing zones in Jeli, Kelantan, Malaysia.

3.1 Resistivity Model of Subsurface Materials

The 2D Res-IP modelling for the two survey lines (SL-1 and SL-2) demonstrates the effectiveness and overall reliability of the geoelectrical acquisition parameters used in this study. Both lines employed a pole–dipole array with an electrode spacing of 5 m, supported by inner and outer cable extensions of 10 m. This configuration provided sufficient depth sensitivity to investigate subsurface variations associated with potential sulphide mineralisation. The specific survey parameters for each profile, along with the corresponding estimates of maximum subsurface lithological unit penetration depth, are summarised in Table 1. SL-1 achieved a maximum depth penetration of approximately 110 m, whereas SL-2 reached slightly deeper depths, up to 120 m. The achieved depths are consistent with expectations for the pole–dipole array at the selected electrode spacing, indicating that the subsurface structures of interest, particularly potential mineralised zones, were effectively imaged within the targeted depth range. The RMS error values obtained from the inversion further support the quality of the models [63]-[66]. For SL-1, RMS errors of 10.9% (resistivity) and 3.8% (chargeability) indicated an acceptable level of misfit between the observed and calculated data, suggesting that the inversion results are well constrained. SL-2 shows slightly higher accuracy for resistivity modelling, with an RMS error of 16.9%, while its chargeability inversion displays a low misfit of 3.4%. Overall, the 2-D Res-IP modelling results from both survey lines provide reliable subsurface images that are suitable for interpreting lithological boundaries, potential fracture zones, and areas of enhanced chargeability that may correspond to massive or disseminated sulphide mineralisation.

Table 1. Survey parameters for SL-1 and SL2

Survey line	Measure mode	Electrode spacing (m)		Maximum depth of penetration (m)	RMS error (%)	
		Inner Cable	Outer Cable		Resistivity (Res)	Chargeability (IP)
SL-1	Res-IP	5	10	100	10.9	3.8
SL-2	Res-IP	5	10	120	16.9	3.4

Figure 4(a) illustrates the 2D resistivity model with topography for survey line 1 (SL-1), while Figure 4(b) depicts the induced polarisation with topography for survey line 1 (SL-1) data. The resistivity values for SL-1 range from 0 Ωm to 26,000 Ωm, and the chargeability values shown span from 0 msec to 40 msec. The maximum measurable depth for both inversion models extends from the surface to 110 meters. Figure 5(a) illustrates the 2D resistivity model with topography for survey line 1 (SL-2), while Figure 5(b) depicts the induced polarisation with topography for survey line 1 (SL-2) data. The resistivity values for SL-2 range from 0 Ωm to 26,000 Ωm, and the chargeability values span from 0 msec to 40 msec. The maximum measurable depth for both inversion models extends from the surface to 110 m.

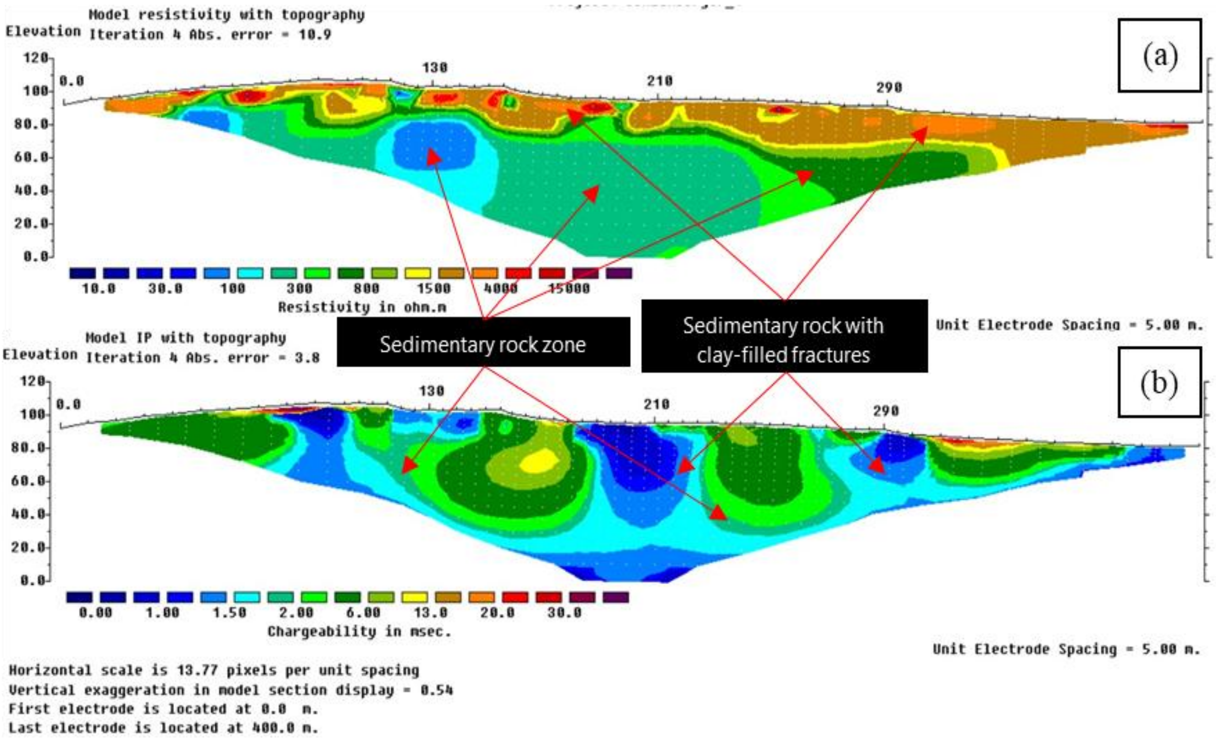

Figure 4. An inversion model of (a) resistivity; (b) Induced polarisation (Res-IP) with topography for SL-1

The inverted Res-IP section, as shown in Figures 4 and 5, reveals laterally continuous and vertically consistent geophysical anomalies. In both profiles, a prominent zone of relatively low resistivity (<300 Ωm) is observed at depths between approximately 30 and 90 m, particularly between lateral distances of 50 to 280 m in SL-1 and 40 to 210 m in SL-2. This conductive zone is spatially coincident with elevated chargeability values at below 10 msec, suggesting the presence of disseminated sulphide minerals rather than simple lithological conductivity associated with clay-rich or water-saturated materials. The coincidence of low resistivity and high chargeability anomalies is significant, as such geophysical signatures are commonly associated with sulphide-bearing mineralised zones in orogenic gold systems. The lateral continuity of this anomaly across both survey lines (SL-1 and SL-2) indicates a structurally controlled feature, potentially related to a fault or shear zone that facilitates hydrothermal fluid flow and sulphide deposition. This interpretation is supported by the sub-vertical geometry of the anomaly and its persistence at depth, which is consistent with mesothermal lode-style gold mineralisation reported in the CBPM. In contrast, the near-surface layer exhibits relatively high resistivity (>2,500 Ωm) and moderate to high chargeability, interpreted as weathered or partially compacted materials with limited mineralisation potential. The intermediate resistivity zone (300 - 2,500 Ωm) likely represents variably weathered bedrock or mixed lithologies, showing weaker and more diffuse IP responses. The deeper conductive zone with minimal chargeability (<2 msec), observed below ~90 m depth, is interpreted as saturated or chemically altered bedrock with limited sulphide content. The consistency of the anomalous low-resistivity and high-chargeability zones across SL-1 and SL-2 strengthens the reliability of the Res-IP interpretation and supports selecting these zones as priority targets for borehole drilling. These features provide a geophysical basis for correlating subsurface lithology with potential sulphide-associated gold mineralisation, which is later validated through borehole data.

Nevertheless, resistivity values alone can be ambiguous, as similar responses may arise from different lithological or structural conditions. To reduce this uncertainty, resistivity data were considered alongside IP results. Low resistivity, paired with low chargeability, is typically consistent with sedimentary rocks. In contrast, high resistivity, coupled with low chargeability, is often associated with metasedimentary units or fractured rocks containing clay infill. In contrast, low resistivity accompanied by elevated chargeability is usually indicative of metallic ore bodies. These comparative relationships are summarised in Table 2 and form the basis for the subsequent discussion of the subsurface conditions.

Table 2. Comparison Res-IP analysis reading

Interpretation of Lithology	Resistivity (Ωm)	Chargeability (msec)
Sedimentary rock	Low	Low
Metasedimentary rock	High	Low
Metallic ore bodies	Low	High

The interpretation of SL-1 highlights a stratified subsurface characterised by high-resistivity values near the surface (upper layer), which transition to moderate- to low-resistivity zones at greater depths. This pattern is consistent with a sedimentary sequence in which relatively compact or less-weathered material overlies more altered or fractured material. The chargeability distribution is generally low across the profile, with only isolated pockets of moderate response, suggesting limited clay within the section. SL-2 reveals a resistivity distribution similar to that observed in SL-1, with low resistivity values on the left flank and progressively higher values toward the right flank. Chargeability across the section remains predominantly low, with only minor zones of moderate response. These results suggest that the left flank is composed predominantly of sedimentary rock. In contrast, the right flank may represent either compact sedimentary rock or metasedimentary rock that has undergone fracturing and subsequent infilling with clay. Table 3 lists the Res-IP parameters and interprets the geophysical characteristics for each survey line.

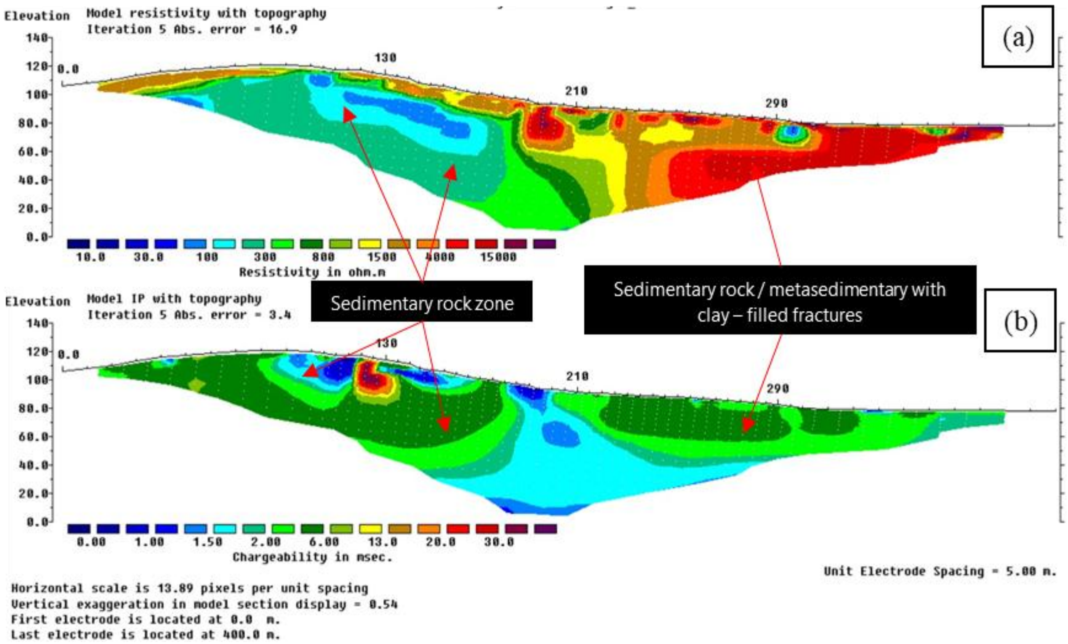

Figure 5. An inversion model of (a) resistivity and (b) induced polarisation (Res-IP) with topography for SL-2

Table 3. Consolidated Res-IP parameters and interpreted geophysical characteristics for each survey line

Survey line	Lithologies interpretation
SL-1	- Sedimentary rock across profile - Upper section interpreted as altered or fractures sedimentary rock - Clay infill within the low chargeability
SL-2	- Left flank indicated as sedimentary rock - Right flank indicated as compact sedimentary rock or metasedimentary rock that has undergone fracturing and subsequent clay infilling

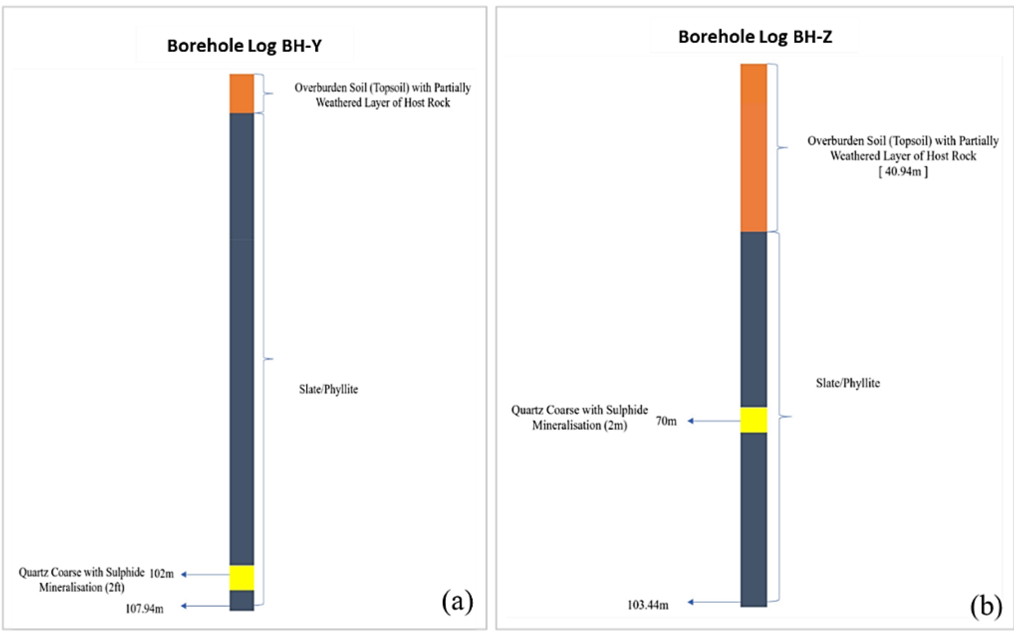

Figure 6. (a) Graphical depiction of the subsurface and borehole conditions observed at BH-Y; (b) Graphical depiction of the subsurface and borehole conditions observed at BH-Z

3.2 Subsurface Lithology

Figure 6(a) graphical depiction of the subsurface and borehole conditions observed at BH-Z. BH-Z was advanced to a final depth of 107.94 m, revealing a stratigraphy beginning with 15 m of overburden soil containing partially weathered host rock, indicative of surface weathering and a transitional zone to competent bedrock. Between 15 and 102 m, the profile is dominated by slate/phyllite, reflecting a thick, continuous sequence of low-grade metamorphic rocks. A narrow 0.6 m interval, located at 102 to 102.6 m, contains quartz-coarse material with sulphide mineralisation, suggesting a minor hydrothermal vein with potential geochemical reactivity. Below this, slate/phyllite persists to the termination depth at 107.94 m, confirming the uniformity of the metamorphic basement. Figure 6(b) shows the borehole conditions for BH-Z. BH-Z was drilled to a total depth of 103.44 m and reveals a stratigraphic profile comprising an extensive overburden layer from 0 to 40.94 m containing soil and partially weathered host rock, indicative of significant near-surface weathering. Beneath this, a continuous slate/phyllite sequence extends from 40.94 to 70 m, representing competent low-grade metamorphic bedrock. A distinct 2 m interval, located between 70 and 72 m, consists of quartz-rich, coarse material with sulphide mineralisation, suggesting a minor hydrothermal vein or mineralised zone with potential geochemical implications. The borehole terminates within slate/phyllite from 72 m to 103.44 m, confirming a predominantly uniform metamorphic basement. This presented profile indicates a subsurface lithology dominated by slate/phyllite, with only a narrow, mineralised discontinuity.

3.3 Resistivity–Lithology Correlation for Gold Mineralisation

The correlation of Res-IP anomalies with borehole data provides a means of validating geophysical interpretations against direct subsurface lithological evidence. While Res-IP anomalies outline variations in resistivity and chargeability across the subsurface, graphical borehole logs serve as ground truth that anchors these responses to specific materials. According to Figure 7, the correlation of BH-Y and BH-Z with SL-2 provides insight into the resistivity and chargeability characteristics of the topsoil and slate units. The topsoil with a partially weathered layer of host rock exhibits resistivity values of 1500 to 2750 Ωm in BH-Y and 1500 to 4000 Ωm in BH-Z, with corresponding chargeability values of 2 to 6 msec and 0.5 to 1.00 msec, respectively. The underlying slate displays resistivity values of 300 to 800 Ωm in BH-Y and 300 to 1150 Ωm in BH-Z, while the chargeability responses remain within similar ranges. By referring to the location and position of borehole drilling aligned with the survey line, as shown in Figure 7, both SL-1 and SL-2 exhibit a pronounced geophysical signature in their basal layers, characterised by low resistivity coupled with high chargeability. This response is commonly associated with sulphide-rich zones, as disseminated or vein-hosted sulphide minerals significantly enhance chargeability while reducing resistivity due to their conductive nature. The consistency of this anomaly across both survey lines suggests a laterally continuous mineralised horizon rather than isolated geophysical noise. In BH-Z, drilled to a depth of 103.44 m, a distinct interval of quartz–coarse-vein material with sulphide mineralisation occurs between 70 and 72 m. This depth coincides with the chargeability enhancement modelled beneath SL-2, confirming that the geophysical anomaly corresponds directly to sulphide-bearing mineralisation. A similar relationship was observed for SL-1: the basal Res-IP anomaly aligns with the quartz–sulphide vein encountered at 102 to 102.6 m in the 107.94 m of deep borehole, demonstrating strong agreement between geophysical predictions and ground-truth lithology. The repeated pattern of low resistivity with high chargeability zones coinciding with sulphide-bearing quartz veins in both boreholes highlights a robust correlation between the two datasets. This convergence supports the interpretation that the anomalies represent structurally controlled hydrothermal mineralisation, consistent with gold-related sulphide systems documented in comparable geological settings [34].

However, in conducting a comprehensive correlation of the geophysical anomalies with the subsurface lithology at the study site, comparable studies in similar geological settings provide valuable reference points. Several researchers have employed the Res-IP method to identify geophysical signatures associated with mineralisation, particularly those linked to gold-bearing zones. For instance, Zaid et al. [13] conducted a Res-IP survey in the Gua Musang area, a region with geological characteristics closely comparable to those of the Jeli district. Their findings further support the applicability of the Res-IP technique in delineating mineralised zones and enhancing the interpretation of geophysical anomalies in structurally complex terrains. Their analysis, based on Res-IP anomalies, reveals two distinct geological zones of large-scale conductive sulphide minerals, as well as regions with low-resistivity sulphide mineralisation, as delineated. They also recorded that the high chargeability zone identified through geophysical anomalies suggests that quartz veins host the sulphide mineralisation zone. Meanwhile, the high resistivity values greater than 2000 Ωm recorded correspond to the basement rock unit. The zones with low resistivity indicate the presence of conductive sulphide mineralisation that hosts the hydrothermal quartz vein through the sheared zone, where gold mineralisation occurs. Other studies conducted by Jegen et al. [65] in Gua Musang and Kuala Krai, Kelantan, reveal that the resistivity patterns identified in Jeli correspond broadly with regional geophysical trends documented across Peninsular Malaysia. However, they also reveal key distinctions that strengthen the interpretation of sulphide-related mineralisation in this study. Previous work in the Gua Musang Formation has demonstrated that sandstone, siltstone, and shale exhibit resistivity values ranging from 500 to 4,000 Ωm, depending on the quartz content and clay fraction. In the present study, the high-resistivity overburden observed in BH-Y and BH-Z (1,500 - 4,000 Ωm) falls within this established range, indicating that the shallow subsurface in Jeli behaves similarly to other CBPM sedimentary and weathered bedrock environments. The other studies in Kuala Krai further report moderate resistivity values (30 - 1,000 Ωm) for schist and granite, governed by mineralogy and moisture conditions. These values closely match the intermediate resistivity ranges (300 - 1,150 Ωm) recorded in the slate/phyllite units in Jeli, reinforcing the consistency of metamorphic basement electrical properties across Kelantan.

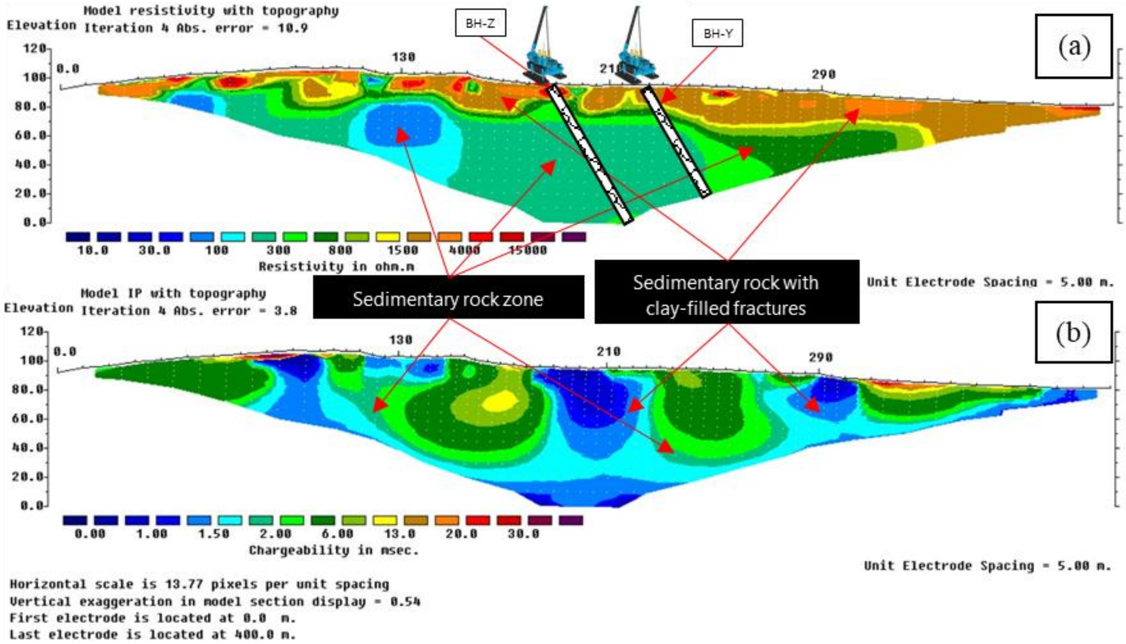

Figure 7. An inversion model of (a) resistivity and (b) induced polarisation (Res-IP) with topography for SL-2

Where Jeli diverges from regional patterns is in the occurrence of deep, low-resistivity (<100 Ωm) and high-chargeability (>100 msec) anomalies, which correlate directly with quartz–sulphide veins intersected in BH-Y and BH-Z. Although previous studies [64] in Kampung Sedar and Kuala Jambu, Tumpat, reported similarly low resistivities (<100 Ωm), these anomalies were attributed to clay-rich alluvium, which is typically shallow and non-mineralised. In contrast, the anomalies in Jeli occur at depths of 70 to 102 meters, exhibit markedly stronger chargeability, and align structurally with hydrothermal vein systems, indicating a mineralogical rather than sedimentological origin. Thus, while the broader resistivity framework in Jeli mirrors regional lithological trends, the unique combination of low resistivity, high chargeability, and borehole-confirmed sulphide intersections distinguishes the study area as a structurally controlled mineralised zone. This comparison validates the thresholds established in this research (<100 Ωm; >100 msec) and demonstrates their geological relevance for gold exploration within the CBPM.

Despite the strong spatial correlation between the Res-IP anomalies and borehole-confirmed sulphide mineralisation, it is necessary to recognise the inherent non-uniqueness of geophysical interpretations [67]- [70]. Low-resistivity and high-chargeability responses may also originate from non-mineral sources, including clay-rich horizons, saline groundwater, graphite-bearing metasedimentary units, or intensely fractured and water-saturated zones. In tropical environments, the presence of deeply weathered regolith further complicates interpretation, as conductive responses may arise from weathering processes unrelated to economic mineralisation. In the present study, several independent lines of evidence reduce the likelihood that the observed anomalies are attributable to such non-mineral causes. First, the anomalous zones are consistently located at depths exceeding 70 meters, well below the typical depth range of clay-rich alluvial or lateritic horizons reported elsewhere in the region. Second, the chargeability values associated with these anomalies (>100 msec) are substantially higher than those commonly observed in clay-dominated or groundwater-controlled environments, which generally exhibit increased conductivity but relatively low chargeability responses. Third, borehole intersections directly confirm the presence of quartz–sulphide veins at depths coincident with the most pronounced geophysical anomalies, providing robust ground-truth validation. Finally, the repeatability and lateral continuity of these anomalies across independent survey lines reduce the likelihood that they represent inversion artefacts or localised lithological noise. Nevertheless, certain uncertainties remain, primarily due to the limited number of boreholes and the inherent resolution constraints of 2D inversion modelling. Additional borehole data and 3D geophysical surveys would further constrain anomaly geometry and improve confidence in resource delineation. Despite these limitations, the results demonstrate that when calibrated with borehole information, combined Res-IP surveys can effectively discriminate sulphide-associated mineralisation from non-mineral-conductive features, even within highly weathered tropical terrains.

3.4 Threshold Values of Subsurface Lithologies

The integration of Res-IP methods and borehole results enables the establishment of threshold ranges for resistivity and chargeability that are representative of the lithologies encountered within the study area (Table 4). These thresholds provide a more reliable framework for distinguishing sedimentary and metamorphic units while reducing uncertainties that arise when interpreting geophysical anomalies. The synthesis of results further indicates the presence of quartz veins and associated anomalies that, although subtle in the Res-IP profiles, correspond with borehole evidence suggesting trace occurrences of gold. This section, therefore, presents the final delineation of resistivity and chargeability ranges and discusses their implications for identifying mineralisation zones. Topsoil is consistently defined by low resistivity values (200 - 400 Ωm) with chargeability responses generally below 2.0 msec, reflecting its unconsolidated and moisture-bearing nature. Overburden containing partially weathered host rock exhibits elevated resistivity (1,500-3,000 Ωm, occasionally up to 4,000 Ωm) and variable chargeability values of 2.0-6.0 msec, reflecting lateritic development and secondary alteration. Limestone shows resistivity values of 500–900 Ωm and chargeability values of 1.25-1.75 msec, indicating a relatively compact but weakly polarizable unit. Slate and phyllite show the widest variation; fresh to moderately weathered material corresponds to resistivity values of 800–1,500 Ωm with chargeability typically between 0.5 and 1.25 msec, while weathered or fractured zones exhibit lower resistivity (300 - 800 Ωm) and higher chargeability values of 2.0 to 6.0 msec due to clay infill and increased surface conduction. The combination of these parameters establishes diagnostic thresholds that enhance lithological discrimination and support the delineation of hydrothermal sulphide mineralisation as seen in the borehole log. Zones of low resistivity (100-300 Ω · m) coupled with elevated chargeability (2.0-6.0 msec) are considered key indicators of sulphide enrichment.

Table 4. Comparison of Res-IP inversion results, highlighting variations in resistivity-chargeability for lithology

Lithology	Resistivity (Ωm)	Chargeability (msec)
Topsoil	200 – 400	1.5 – 2.0
Topsoil with partially weathered host rock	1500 – 3000 (up to 4000)	2.0 – 60
Limestone	500 – 900	1.25 – 1.75
Slate (fresh to moderately weathered)	800 – 1500	0.5 – 1.25
Slate (weathered/fractured)	300 – 800	2.0 – 6.0

These thresholds have important implications for mineralisation studies in the area. Zones characterised by low resistivity (100–300 Ωm) and elevated chargeability (2.0–6.0 msec) can be reliably associated with sulphide enrichment, particularly were corroborated by borehole evidence of quartz veins with sulphide mineralisation. By contrast, high-resistivity and low-chargeability zones are more consistent with compact, unmineralized lithologies such as fresh slate. The ability to discriminate between these responses reduces the ambiguity inherent in geophysical interpretation and provides a practical guide for delineating prospective targets. In this context, the integrated thresholds serve to differentiate complex lithological units within hydrothermal sulphide-bearing quartz veins. To support the selection of resistivity threshold values, a comparative synthesis of resistivity ranges reported in Malaysian case studies was undertaken, as summarised in Table 5. These studies represent independent investigations conducted under diverse geological and hydrogeological settings. Although the reported resistivity values are inherently site-specific, a clear degree of overlap is observed among the documented ranges, providing a rational basis for defining representative threshold intervals. Accordingly, the threshold values adopted in this study were selected within the convergent bands of the reported resistivity ranges rather than at their extreme limits. This approach ensures that the selected thresholds remain physically plausible, regionally relevant, and consistent with established empirical observations, thereby strengthening the reliability of the subsurface interpretations.

Table 5. Comparison of Res-IP inversion results with others case study

Lithology	Resistivity (Ωm)	Resistivity from past researchers (Ωm)	References
Topsoil	200 – 400, and 1500 – 3000 (up to 4000) for partially weathered host rock	50 – 400 (moist)	Abubakar et al. [67]
		400 – 5000 (dry)	
		5000 – 20000 (very dry soil/weathered soil)	
		100 – 13000	Tan et al. [68]
		130 – 1400	Ismail and Yaacob [69]
		200 – 600	Daud et al. [25]
		350 – 800	Islami et al. [70]
		450 – 1000	Samsudin et al. [71]
Limestone	500 – 900	200 – 600	Liew et al. [72]
		800 – 5000	Nordiana et al. [73]
		1200 – 3000 (fresh), 125 – 500 (weathered)	Che Mamat et al. [74]

3.5 Sensitivity Assessment of Subsurface Lithologies

A sensitivity assessment was conducted to evaluate the robustness of subsurface interpretations with respect to uncertainties in resistivity threshold values. Electrical resistivity in geological materials is inherently variable, particularly under tropical conditions where moisture content, weathering intensity, and groundwater saturation exhibit strong spatial heterogeneity. To address this uncertainty, resistivity thresholds were systematically varied within established intervals to assess whether the interpreted lithological boundaries remain stable under plausible subsurface conditions. The assessment was implemented by varying resistivity values while maintaining constant survey geometry, electrode configuration, inversion parameters, and topographic corrections. For each lithological unit, end-member scenarios representing lower and upper resistivity bounds were examined, corresponding to realistic material states such as saturated versus less saturated topsoil, weathered versus fresh limestone, and fractured versus relatively intact slate. The resulting inversion models were evaluated based on anomaly persistence, boundary continuity, depth consistency, and spatial geometry. Results indicate that the primary lithological interpretations remain consistent across the tested resistivity ranges, with only minor boundary shifts observed in transitional zones. In particular, the slate resistivity thresholds defined using a sensitivity-based approach (300–800 Ωm and 800–1500 Ωm) yielded stable, coherent subsurface interpretations, confirming their robustness. Overall, the assessment demonstrates that the adopted resistivity thresholds provide a reliable basis for interpretation, with outcomes governed by resistivity contrasts and spatial continuity rather than isolated threshold selection.

4. Conclusions

This study demonstrates that integrating electrical Res-IP with borehole validation provides a reliable method for identifying sulphide-associated gold mineralisation in the Jeli region of Kelantan. The Res-IP results reveal that zones with resistivity values below 100 Ωm and chargeability values exceeding 100 msec consistently correspond to sulphide-bearing quartz veins. Early predictions and interpretations derived from Res-IP data help prevent damage to soil structure by providing accurate information on subsurface conditions, thereby enabling engineers, geologists, and researchers to determine appropriate materials and design requirements. These geophysical anomalies are confirmed by borehole intersections at 70 to 72 m in BH-Z and 102 to 102.6 m in BH-Y, establishing a clear depth-controlled relationship between the geoelectrical anomalies and the actual lithological conditions. The quantitative agreement between the inversion models and borehole data reduces the non-uniqueness typically associated with Res-IP interpretation, demonstrating that these thresholds are robust indicators of mineralisation under tropical weathering conditions. The study further establishes resistivity ranges for the local stratigraphy: 1,500 to 4,000 Ωm for the overburden and 300 to 1,150 Ωm for slate/phyllite, contributing a region-specific geoelectrical reference for the CBPM.

Overall, this study provides several important contributions toward establishing a robust integrated exploration framework in which geophysical methods are systematically validated through borehole observations:

i. It demonstrates a strong spatial and numerical correspondence between Res-IP anomalies and borehole-confirmed quartz–sulphide veins, thereby affirming the geological validity of the identified geoelectrical signatures.
ii. It reduces interpretational ambiguity by calibrating geophysical responses directly against lithological evidence, thereby addressing the inherent non-uniqueness of resistivity and induced polarisation datasets.
iii. It develops a region-specific geoelectrical characterisation for the CBPM, enhancing the reliability of Res-IP methods in structurally controlled hydrothermal gold systems.
iv. It advances exploration efficiency by providing an integrated methodological framework that improves drill-target prioritisation and minimises unnecessary drilling expenditures.

This study is limited by its reliance on two-dimensional (2D) geophysical models and validation from only two boreholes within a localised area. Although strong correlations were observed between Res-IP anomalies and sulphide-bearing zones, the use of 2D inversion may oversimplify subsurface geometries in structurally complex gold systems. Consequently, the calibrated resistivity–chargeability thresholds are site-specific and may not be directly transferable to other tropical settings. Expanded geophysical coverage incorporating additional Res-IP survey lines, three-dimensional inversion modelling, and further drilling would improve structural resolution, enhance continuity assessment of mineralised zones, and strengthen the broader applicability of the results.

Acknowledgements

The authors would like to express their sincere gratitude to Faculty of Civil Engineering Technology, Universiti Malaysia Pahang Al-Sultan Abdullah for the contributed in supporting to the completion of this manuscript. The authors sincerely thank the anonymous reviewers for their constructive comments and valuable suggestions, which significantly improved the quality of this manuscript.

Funding

The authors would like to express their gratitude to Universiti Malaysia Pahang Al-Sultan Abdullah (UMPSA) for provided the Grant (RDU243007 – Geran Unggul, RDU252401/UIC250802 – Geran Padanan Industri & UIC UIC251518 – Geran Industri), also for the continuous support in providing research facilities and resources throughout the completion of this study.

Declaration of Competing Interests

The authors declare no conflicts of interest.

Credit Authorship Contribution Statement

O. C. Wee (Conceptualization; Formal analysis; Methodology; Writing - original draft)
M. F. Ishak (Conceptualization; Supervision; Resources; Data Validation; Writing - review & editing)
S. Daud (Data Collection; Data curation; Investigation; Writing - review & editing)
P. I. Ismi (Methodology; Data Collection; Writing - review & editing)
Y. A. Sari (Methodology; Analysis; Writing - review & editing)

Availability of Data and Materials

The data supporting this study’s findings are available on request from the corresponding author.

Ethics Declarations

This study did not involve human participants or animals. Ethical approval was therefore not required.

Generative Artificial Intelligence Declarations

The authors claim that artificially intelligent-assisted technologies, such as generative AI, were not used to generate content, ideas, or theories. We have just utilised AI to enhance readability and refine the language. This was used with extreme human control and oversight. The authors take full responsibility for reviewing and approving the content.

References

[1] K. S. Ariffin and N. Hewson, "Gold-related sulfide mineralization and ore genesis of the penjom gold deposit, Pahang, Malaysia," *Resources Geology*, vol. 57, pp. 149–169, 2007, https://doi.org/10.1111/j.1751-3928.2007.00014.x.

[2] E. B. Yeap, "Tin and gold mineralization in Peninsular Malaysia and their relationships to the tectonic development," *Journal of Southeast Asian Earth Sciences*, vol. 8, nos. 1–4, pp. 329–348, 1993, https://doi.org/10.1016/0743-9547(93)90035-N.

[3] A. K. Lee, Y. Khong, and O. W. Hock, "Gold mineralisation and prospects in North Pahang," in *Proceeding of Bicentennial Gold '88, Extended Abstracts Poster Programme*, vol. 1, pp. 238–242, 1988.

[4] N. Muda, N. R. Ainuddeen, H. Ismail, and M. R. Umor, "Modeling of gold production in Malaysia," *AIP Conference Proceedings*, vol. 1522, pp. 1179–1184, 2013, https://doi.org/10.1063/1.4801265.

[5] A. F. Yusoff, J. H. A. Aziz, and M. H. Roselee, "Mineralogy and geochemistry of gold mineralization at southern part of Ulu Sokor gold deposit, Kelantan, Malaysia," *Sains Malaysiana*, vol. 51, no. 12, pp. 3865–3877, 2022, https://doi.org/10.17576/jsm-2022-5112-01.

[6] M. G. Tagwai, O. A. Jimoh, K. S. Ariffin, and M. F. A. Razak, "Investigation based on quantified spatial relationships between gold deposits and ore genesis factors in northeast Malaysia," *Journal of Spatial Science*, vol. 66, no. 2, pp. 229–252, 2019, https://doi.org/10.1080/14498596.2019.1606742 .

[7] J. S. Kayode, M. H. Arifin, M. B. I. Basori, and M. N. M. Nawawi, "Gold prospecting mapping in the Peninsular Malaysia gold belts," *Pure Applied Geophysics*, vol. 179, pp. 3295–3328, 2022, https://doi.org/10.1007/s00024-022-03121-w.

[8] M. H. Arifin, J. S. Kayode, M. K. Izwan, H. A. H. Zaid, and H. Hussin, "Data for the potential gold mineralization mapping with the applications of Electrical Resistivity Imaging and Induced Polarization geophysical surveys," *Data in Brief*, vol. 22, pp. 830–835, 2019, https://doi.org/10.1016/j.dib.2018.12.086.

[9] K. S. Ariffin, "Mesothermal Lode Gold Deposit Central Belt Peninsular Malaysia," in Earth Sciences, I. A. Dar, Ed. Rijeka, Croatia: *InTech*, 2012, pp. 313–342, https://doi.org/10.5772/26179.

[10] C. Makoundi, K. Zaw, R. R. Large, S. Meffre, C. K. Lai, and T. G. Hoe, "Geology, geochemistry and metallogenesis of the Selinsing gold deposit, central Malaysia," *Gondwana Research*, vol. 26, no. 1, pp. 241–261, 2014, https://doi.org/10.1016/j.gr.2013.08.023

[11] Z. Endut, T. Ng, J. H. A. Aziz, and G. Teh, "Structural analysis and vein episode of the Penjom gold deposit, Malaysia: Implications for gold mineralisation and tectonic history in the central belt of Malaysia," *Ore Geology Reviews*, no. 69, pp. 157–173, 2015, https://doi.org/10.1016/j.oregeorev.2015.02.012.

[12] A. B. Pour and M. Hashim, "Structural mapping using PALSAR data in the Central Gold Belt, Peninsular Malaysia," *Ore Geology Reviews*, vol. 64, no. 1, pp. 13–22, 2015, https://doi.org/10.1016/j.oregeorev.2014.06.011.

[13] H. A. H. Zaid, M. H. Arifin, J. S. Kayode, M. B. I. Basori, M. R. Umor, and S. H. Hazim, "Application of 2-D Electrical Resistivity Imaging, and Induced Polarization Methods for Delineating Gold Mineralization at Felda Chiku 3, Kelantan, Malaysia," *Sains Malaysiana*, vol. 52, no. 1, pp. 305–320, 2023, https://doi.org/10.17576/jsm-2023-5201-25.

[14] P. Sono, B. Nthaba, E. M. Shemang, B. Kgosidintsi, and T. Seane, "An integrated use of induced polarization and electrical resistivity imaging methods to delineate zones of potential gold mineralization in the Phitshane Molopo area, Southeast Botswana," *Journal of African Earth Sciences*, vol. 174, p. 104060, pp. 1-13, 2021, https://doi.org/10.1016/j.jafrearsci.2020.104060.

[15] B. D. Lenhare and C. A. Moreira, "Geophysical prospecting over a meta-ultramafic sequence with indicators of gold mineralization in Rio Grande do Sul State, Southernmost Brazil," *Pure and Applied Geophysics*, no. 177, pp. 5367–5383, 2020, https://doi.org/10.1007/s00024-020-02559-0 .

[16] S. R. Mashhadi, M. Nikfarjam, and A. K. Mehrnia, "Reinterpretation of resistivity and induced polarization data to explore gold mineralization zones at Zarzima prospect, Iran," *Acta Geologica Slovaca*, vol. 12, no. 1, pp. 15–22, 2020.

[17] A. N. Fon, V. B. Che, and C. E. Suh, "Application of electrical resistivity and chargeability data on a GIS platform in delineating auriferous structures in a deeply weathered lateritic terrain, eastern Cameroon," *International Journal of Geosciences*, vol. 3, no. 5, pp. 960-971, 2012, https://doi.org/10.4236/ijg.2012.325097.

[18] R. J. Irvine and M. J. Smith, "Geophysical exploration for epithermal gold deposits," *Journal of Geochemical Exploration*, vol. 36, no. 1–3, pp. 375–412, 1990, https://doi.org/10.1016/0375-6742(90)90061-E.

[19] P. Kearey, M. Brooks, and I. Hill, "*An Introduction to Geophysical Exploration*," 3rd ed. Oxford, U.K.: Blackwell Science Ltd., 2002.

[20] S. R. Mashhadi and H. Ramazi, "The application of resistivity and induced polarization methods in identification of skarn alteration haloes: A case study in the Qale-Alimoradkhan area," *Journal of Environmental and Engineering Geophysics*, vol. 23, no. 3, pp. 363–368, 2018, https://doi.org/10.2113/JEEG23.3.363.

[21] C. A. Moreira, K. Borssatto, L. M. Ilha, S. F. D. Santos, and F. T. G. Rosa, "Geophysical modeling in gold deposit through DC resistivity and induced polarization methods," *REM-International Engineering Journal*, vol. 69, no. 3, pp. 293–299, 2016, https://doi.org/10.1590/0370-44672016690001 .

[22] S. Salarian, O. Asghari, M. Abedi, and S. K. Alilou, "Geostatistical-based geophysical model of electrical resistivity and chargeability to image Cu mineralization in Ghalandar deposit, Iran," *International Journal of Mining Geo-Engineering*, vol. 52, no. 2, pp. 153–160, 2019, https://doi.org/10.22059/ijmge.2019.275091.594780 .

[23] M. F. Ishak, M. F. Zolkepli, S. Daud, N. Z. M. Yunus, and A. S. A. Rashid, "The application of unmanned aerial vehicle (UAV) for slope mapping at Gambang Damai residents, Pahang: A Case Study," *International Journal of Integrated Engineering*, vol. 15, no. 2, pp. 219–227, 2023, https://doi.org/10.30880/ijie.2023.15.02.021.

[24] S. Daud, M. F. Ishak, P. I. Ismi, and M. F. Zolkepli, "Investigation of potential groundwater sources using electrical resistivity imaging for industrial facilities in Gebeng, Kuantan, Malaysia: A case study," *Warta Geologi*, vol. 51, no. 2, pp. 77–85, 2025, https://doi.org/10.7186/wg512202502

[25] S. Daud, M. F. Ishak, P. I. Ismi, N. Muhammad, and S. Ghazali, "Granite exploration by using resistivity and induced polarization imaging in western granite belt, Pendang, Kedah, Malaysia," *Smart Construction and Sustainable Cities*, vol. 3, no. 23, pp. 1-16, 2025, https://doi.org/10.1007/s44268-025-00067-5.

[26] D. T. Kieu and A. Kepic, "Integration of borehole data in geophysical inversion using Fuzzy clustering," *ASEG Extended Abstracts*, vol. 2018, no. 1, pp. 1–6, 2018, https://doi.org/10.1071/aseg2018abp083.

[27] A. Bello, N. M. Muztaza, I. A. Abir, M. T. Zakaria, and J. Bello, "Geophysical performance of subsurface characterization for site suitability in construction purpose," *Physics and Chemistry of the Earth, Parts A/B/C*, vol. 128, p. 1-11, 2022, https://doi.org/10.1016/j.pce.2022.103296.

[28] M. D. Dick, A. A. Bery, A. S. Akingboye, K. R. Ekanem, E. Moses, and S. Purohit, "Subsurface lithological characterization via machine learning-assisted electrical resistivity and SPT-N modeling: A Case Study from Sabah, Malaysia," *Earth Systems and Environment*, vol. 9, no. 3, pp. 2457–2480, 2025, https://doi.org/10.1007/s41748-024-00516-8.

[29] T. Unjah, I. Komoo, and H. Mohamad, "Pengenalpastian sumber warisan geologi di Negeri Kelantan," *in Geological Heritage of Malaysia (Geoheritage Mapping and Geosite Characterization), LESTARI UMK*, pp. 111–126, 2001.

[30] G. S. Heng, T. G. Hoe, and W. F. W. Hassan, "Gold mineralization and zonation in the state of Kelantan," *Geological Society of Malaysia Bulletin*, pp. 129–135, 2006.

[31] D. Adriansyah, I. Busu, H. Eva, and M. Muqtada, "Geoheritage as the basis for geotourism development: A case study in Jeli district, Kelantan, Malaysia," *Geojournal of Tourism and Geosites*, vol. 15, no. 1, pp. 25–43, 2015.

[32] Z. M. Nizam, H. Obiya, A. T. S. Azhar, Z. M. N. Hidayat, M. Aziman, J. Amir, I. M. Fakhrurrazi, "The Correlation Between Electrical Resistivity Tomography and Borehole Data at a Coastal Semi Developed Area," *International Journal of Integrated Engineering*, vol. 18, no. 3, pp. 243–256, 2026, https://doi.org/10.30880/ijie.2026.18.03.016.

[33] N. Sulaiman, N. Sulaiman, H. Hussin, A. M. A. Bahar, and W. S. Udin, "Diversification of igneous rocks and geoheritage values in Pergau, Jeli diversification of igneous rocks and geoheritage values in Pergau, Jeli Kelantan," *IOP Conference Series: Earth and Environmental Science*, no. 549, pp. 1-6, 2020, https://doi.org/10.1088/1755-1315/549/1/012020 .

[34] S. Yusoff, B. Pradhan, M. A. Manap, and H. Z. M. Shafri, "Regional gold potential mapping in Kelantan (Malaysia) using probabilistic based models and GIS," *Open Geosciences*, vol. 7, no. 1, pp. 149–161, 2015, https://doi.org/10.1515/geo-2015-0012.

[35] S. MacDonald, "*The geology and mineral resources of North Kelantan and North Trengganu*," District Memoir 1, Geological Survey of Malaysia, Ipoh, Malaysia, 1967.

[36] D. Rishworth, "The upper mesozoic terrigenous gagau group of Peninsular Malaysia," *Geological Society of Malaysia*, pp. 1–78, 1974.

[37] W. F. W. Hassan and H. S. Purwanto, "Type deposits of primary gold mineralization in the Central Belt of Peninsular Malaysia," *in Geological Society of Malaysia Annual Geological Conference, Kota Bharu, Kelantan: Geological Society of Malaysia*, 2002.

[38] L. H. Teoh, A. K. Lee, and K. Y. Foo, "*Gold Mineralization and Prospects in Kelantan*," Minerals and Geoscience Department Malaysia (unpublished report), 1987.

[39] C. L. Heng and D. S. Singh, "The nature and potential of gold mineralization in Kelantan, Peninsular Malaysia," *Geological Society of Malaysia Bulletin*, vol. 1, no. 19, pp. 431–440, 1986.

[40] L. H. Chu, "*Exploration in the Sok Base Metal Prospect, Kelantan*," Geological Survey Malaysia Report (unpublished), 1983.

[41] C. S. Hutchinson and D. N. Tan, "*Geology of Peninsular Malaysia*," Kuala Lumpur: The University of Malaya and The Geological Society of Malaysia, 2009, p. 479.

[42] M. S. Sulaiman, W. S. Udin, M. A. Khan, N. Sulaiman, R. Ismail, and A. Bahar, "Analysis of drainage pattern and its relationship with gold potential in Batu Melintang, Jeli, Kelantan," *IOP Conference Series: Earth and Environmental Science*, vol. 842, no. 1, pp. 1-6, 2021, https://doi.org/10.1088/1755-1315/842/1/012043.

[43] A. Marciniak, S. Kowalczyk, T. Gontar, et al., "Integrated geophysical imaging of a mountain landslide - a case study from the Outer Carpathians" *Journal Applied Geophysics*, vol. 191, p. 1-12, 2021, https://doi.org/10.1016/j.jappgeo.2021.104364.

[44] D. F. Rucker, C. H. Isai, K. C. Carroll, et al., “Bedrock architecture, soil texture, and hyporheic zone characterization combining electrical resistivity and induced polarization imaging,” *Journal Applied Geophysics*, vol. 188, p. 1-12, 2021, 10.1016/j.jappgeo.2021.104306.

[45] M. H. Z. Abidin, R. Saad, F. Ahmad, D. C. Wijeyesekera, and M. F. T. Baharuddin, “Application of Geophysical Methods in Civil Engineering,” *in Proc. Malaysian Technical Universities International Conference on Engineering & Technology* (MUiCET 2011), Batu Pahat, Johor, Malaysia, 2011, pp. 1–12.

[46] M. H. Loke, “*Tutorial: 2D and 3D electrical imaging surveys*,” Geotomo Software, 2012. [Online]. Available: https://geotomosoft.com

[47] M. Loke and R. D. Barker, “Rapid least-squares inversion of apparent resistivity pseudosections using a quasi-newton method,” *Geophysical Prospecting*, vol. 44, pp. 131–152, 1996. https://doi.org/10.1111/j.1365-2478.1996.tb00142.x.

[48] A. Upadhyay, A. Singh, K. P. Panda, and S. P. Sharma, “Delineation of gold mineralization near Lawa Village, North Singhbhum Mobile Belt, India, using electrical resistivity imaging, self-potential and very low frequency methods,” *Journal Applied Geophysics*, vol. 172, p. 1-13, 2020, https://doi.org/10.1016/j.jappgeo.2019.103902.

[49] M. D. Babu, A. Manglik, S. Thiagarajan, and M. Suresh, “Electrical resistivity image of a basement ridge in the foreland central Ganga basin,” *Journal Applied Geophysics*, vol. 179, p. 1-9, 2020, https://doi.org/10.1016/j.jappgeo.2020.104097 .

[50] S. Li, S. Xu, L. Nie, et al., “Assessment of electrical resistivity imaging for pre-tunneling geological characterization – A case study of the Qingdao R3 metro line tunnel,” *Journal Applied Geophysics*, vol. 153, pp. 38–46, 2018, https://doi.org/10.1016/j.jappgeo.2018.03.024.

[51] P. I. Ismi, M. F. Ishak, and S. Daud, “Prefeasibility mining studies by using electrical resistivity imaging (ERI) in Keratong, Pahang,” *Bulletin of the Geological Society of Malaysia*, vol. 80, pp. 83-93, 2025, https://doi.org/10.7186/bgsm80202506.

[52] R. C. Smith and D. B. Sjogren, “An evaluation of electrical resistivity imaging (ERI) in quaternary sediments, Southern Alberta, Canada,” *Geosphere*, vol. 2, no. 6, pp. 287–298, 2006, https://doi.org/10.1130/GES00048.1.

[53] L. Marescot, R. Monnet, and D. Chapellier, “Resistivity and induced polarization surveys for slope instability studies in the Swiss Alps,” *Engineering Geology*, vol. 98, no. 1–2, pp. 18–28. 2008, https://doi.org/10.1016/j.enggeo.2008.01.010.

[54] P. V. Sharma, *Environmental and Engineering Geophysics*. Cambridge, U.K.: Cambridge University Press, 1997.

[55] K. Spitzer and M. Chouteau, “A DC resistivity and IP borehole survey at the Casa Berardi gold mine in Northwestern Quebec,” *Geophysics*, vol. 68, no. 2, pp. 453–463, 2003, https://doi.org/10.1190/1.1567221.

[56] J. M. Reynolds, *An Introduction to Applied and Environmental Geophysics*, 2nd ed. Chichester, West Sussex, U.K.: Wiley-Blackwell, 2011.

[57] M. H. Arifin, J. S. Kayode, K. I. Ismail, M. Abdullah, A. Embrandiri, and S. M. Nazer Azmi, “Data for the industrial and municipal environmental wastes hazard contaminants assessment with integration of RES2D techniques and Oasis Montaj software,” *Data in Brief*, vol. 33, pp. 1-8, p. 106595, 2020, https://doi.org/10.1016/j.dib.2020.106595.

[58] Z.-X. Zhang, “Rock drilling and boring,” in *Rock Fracture and Blasting: Theory and Applications*. Oxford, U.K.: Butterworth-Heinemann, 2016, pp. 155–175, https://doi.org/10.1016/B978-0-12-802688-5.00007-5.

[59] M. A. Olade, *Introduction to mineral deposits geology: including exploration, mining and mineral economics*. Pearland, TX, USA: Prescott Publishers, 2022.

[60] M. Cozzolino, P. Mauriello, M. Moisidi, and F. Vallianatos, “A probability electrical resistivity tomography imaging of complex tectonic features in the kissamos and paleohora urban areas, western crete (Greece),” *Annals of Geophysics*, vol. 62, no. 6, pp. 1–19, 2020, https://doi.org/10.4401/ag-7938.

[61] Y. Munko-Abo and A. Zakari, “The use of electrical resistivity imaging and induced polarization surveys to investigate underground tunnels filled with water, case study—Akoon, Tarkwa-Ghana,” *Journal of Umm Al-Qura University for Engineering and Architecture*, vol. 16, no. 2, pp. 370–378, 2025, https://doi.org/10.1007/s43995-025-00112-5.

[62] P. M. Soupios, P. Georgakopoulos, N. Papadopoulos, et al., “Use of engineering geophysics to investigate a site for a building foundation,” *Journal of Geophysics and Engineering*, vol. 4, no. 1, pp. 94–103, 2007, https://doi.org/10.1088/1742-2132/4/1/011.

[63] S. Daud, M. F. Ishak, Q. H. Hussein, P. I. Ismi, and M. F. Zolkepli, “Integrating Forensic Analysis and Sustainable Design for Slope Stabilization: A case study using waste tire-filled gabion structure (WTFGS),” *International Journal of Integrated Engineering*, vol. 17, no. 9, pp. 446–462, 2025, https://doi.org/10.30880/ijie.2025.17.09.031.

[64] Z. M. Nizam, A. T. S. Azhar, M. Aziman, Z. M. N. Hidayat, J. A. Aziz, and N. M. N. Amri, “Assessing the Impact of Lithological and Geological Features on Electrical Resistivity Tomography (ERT) at Kelantan River Basin, Malaysia,” *International Journal of Integrated Engineering*, vol. 16, no. 4, pp. 113–123, 2024, https://doi.org/10.30880/ijie.2024.16.04.014.

[65] M. D. Jegen, R. W. Hobbs, P. Tarits, and A. Chave, “Joint inversion of marine magnetotelluric and gravity data incorporating seismic constraints: Preliminary results of sub-basalt imaging off the Faroe Shelf,” *Earth and Planetary Science Letters*, vol. 282, no. 1–4, pp. 47–55, 2009, https://doi.org/10.1016/j.epsl.2009.02.018.

[66] N. E. H. Ismail, S. H. Taib, and F. A. M. Abas, “Slope monitoring: an application of time - lapse electrical resistivity imaging method in Bukit Antarabangsa, Kuala Lumpur,” *Environmental Earth Sciences*, vol. 78, no. 14, pp. 1–14, 2019, https://doi.org/10.1007/s12665-018-8019-9.

[67] S. Abubakar, I. A. Abir, R. A. Rahman, and N. M. Muztaza, "Landslide susceptibility analysis of Kamping Iboi, Muda River Basin, Kedah, Malaysia using remote sensing, 2D - resistivity and GPR," *Advances in Space Research*, vol. 76, pp. 4106–4124, 2025, https://doi.org/10.1016/j.asr.2025.07.052.

[68] S. N. M. A. Tan, M. E. Tonnizam, R. Saad, et al., "Correlation of resistivity value with geotechnical N-value of sedimentary area in Nusajaya, Johor, Malaysia," *Journal of Physics: Conference Series*, vol. 995, pp. 1–13, 2018, https://doi.org/10.1088/1742-6596/995/1/012079.

[69] N. I. Ismail and W. Z. W. Yaacob, "Application of electrical resistivity tomograph (ERT) for slope failure investigation: a case study from Kuala Lumpur," *Jurnal Teknologi (Sciences & Engineering)*, vol. 80, pp. 79–86, 2018, https://doi.org/10.11113/jt.v80.11624.

[70] N. Islami, S. H. Taib, I. Yusoff, and A. A. Ghani, "Integrated geoelectrical resistivity & hydrogeochemical method for delineating and mapping heavy metal zone in aquifer system," *Environmental Earth Sciences*, vol. 77, no. 383, pp. 1–18, 2018, https://doi.org/10.1007/s12665-018-7574-4.

[71] A. R. Samsudin, U. Hamzah, A. G. Rafek, and R. Yaacup, "Application of geoelectrical resistivity imaging for site investigation," *Geological Society of Malaysia Annual Geological Conference 2000*, pp. 375–379.

[72] S. S. Liew, C. N. Tiu, F. W. Chee, and H. Y. Yong, "2D electrical resistivity tomograph (ERT) & induced polarisation (IP) survey on detection of karst features and connectivity of solution channel," *EAGE - GSM 2nd Asia Pacific Meeting on Near Surface Geoscience & Engineering*, pp. 1–4, 2019, https://doi.org/10.7186/bgsm58201209.

[73] M. M. Nordiana, R. Saad, M. N. M. Nawawi, I. N. Azwin, and E. T. Mohamad, "Case study: Shallow subsurface geology mapping using 2-D resistivity imaging with EHR technique," *Asia - Pacific Chemical, Biological & Environmental Engineering Society Procedia*, vol. 5, pp. 134–140, 2013, https://doi.org/10.1016/j.apcbee.2013.05.024.

[74] R. Che Mamat, A. Ramli, A. H. Abd Aziz, M. D. H. Azhari, and A. Jackson, "A comparative analysis of fly ash enhanced micropiles in sustainable foundation systems," *Smart and Green Materials*, vol. 2, no. 1, pp. 35–46, 2025, https://doi.org/10.70028/sgm.v2i1.35.